Food & Function

Accepted Manuscript

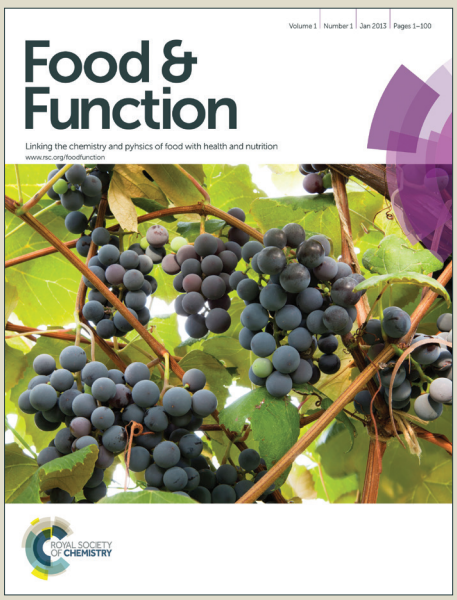

This is an *Accepted Manuscript*, which has been through the Royal Society of Chemistry peer review process and has been accepted for publication.

Accepted Manuscripts are published online shortly after acceptance, before technical editing, formatting and proof reading. Using this free service, authors can make their results available to the community, in citable form, before we publish the edited article. We will replace this *Accepted Manuscript* with the edited and formatted *Advance Article* as soon as it is available.

You can find more information about *Accepted Manuscripts* in the Information for Authors.

Please note that technical editing may introduce minor changes to the text and/or graphics, which may alter content. The journal's standard Terms & Conditions and the Ethical guidelines still apply. In no event shall the Royal Society of Chemistry be held responsible for any errors or omissions in this *Accepted Manuscript* or any consequences arising from the use of any information it contains.

ROYAL SOCIETY OF CHEMISTRY

www.rsc.org/foodfunction

Curcumin prevents cisplatin-induced decrease in the tight and adherens junctions: relation to oxidative stress.

Joyce Trujillo[a,*], Eduardo Molina-Jijón[b,*], Omar Noel Medina-Campos[a], Rafael Rodríguez-Muñoz[b], José Luis Reyes[b], María L Loredo[c], Diana Barrera-Oviedo[d], Enrique Pinzón[e], Daniela Saraí Rodríguez-Rangel[a], José Pedraza-Chaverri[a,**].

[a]Department of Biology, Faculty of Chemistry, National Autonomous University of Mexico (UNAM), 04510 University City, D.F., Mexico.

[b]Department of Physiology, Biophysics and Neurosciences. Center for Research and Advanced Studies of the National Polytechnic Institute (Cinvestav-IPN), Mexico City, 07360. Mexico.

[c]School of Medicine, Panamericana University, Mexico City, 03920, Mexico.

[d]Department of Pharmacology and [e]Animal Care Unit, Faculty of Medicine, National Autonomous University of Mexico (UNAM), University City, 04510. Mexico.

*Both authors contributed equally to this work and should be considered as firsts authors.

****Corresponding author:**

José Pedraza-Chaverri, Laboratory 209, Building F, Faculty of Chemistry, Department of Biology, National Autonomous University of Mexico (UNAM), University City, 04510, D.F., México.

Phone/Fax: +52 55 5622-3878. E-mail: pedraza@unam.mx

Abstract

Curcumin is a polyphenol and cisplatin is an antineoplasic agent that induces nephrotoxicity associated to oxidative stress, apoptosis, fibrosis and decrease in renal tight junction (TJ)

proteins. The potential effect of curcumin against alterations in TJ structure and function has not been evaluated in cisplatin-induced nephrotoxicity. The present study explored whether curcumin is able to prevent the cisplatin-induced fibrosis and decreased expression of the TJ and adherens junction (AJ) proteins occludin, claudin-2 and E-cadherin in cisplatin-induced nephrotoxicity. Curcumin (200 mg/kg) was administered in three doses, and rats were sacrificed 72 h after cisplatin administration. Curcumin was able to scavenge, in a concentration-dependent way, superoxide anion, hydroxyl radical, peroxyl radical, singlet oxygen, peroxynitrite anion, hypochlorous acid and hydrogen peroxide. Cisplatin-induced renal damage was associated with alterations in plasma creatinine, expression of neutrophil gelatinase-associated lipocalin and of kidney injury molecule-1, histological damage, increase in apoptosis, fibrosis (evaluated by transforming growth factor β1, collagen I and IV and α-smooth muscle actin expressions), increase in oxidative/nitrosative stress (evaluated by Hsp70/72 expression, protein tyrosine nitration, superoxide anion production in isolated glomeruli and proximal tubules, and protein levels of NADPH oxidase subunits $p47^{phox}$ and $gp91^{phox}$, protein kinase C β2, and Nrf2) as well as by decreased expression of occludin, claudin-2, β-catenin and E-cadherin. Curcumin treatment prevented all the above-described alterations. The protective effect of curcumin against cisplatin-induced fibrosis and decreased proteins of the TJ and AJ was associated with the prevention of glomerular and proximal tubular superoxide anion production induced by NADPH oxidase activity.

Key words: occludin, claudin-2, E-cadherin, curcumin, cisplatin, superoxide production.

Introduction

The renal tubule plays a major role in the reabsorption of water and solutes in the nephron. Tight junction (TJ) restricts paracellular transport of solutes and water, and adherens junction (AJ) regulate transcellular and paracellular transport. Several integral membrane proteins

have been identified as components of TJ strands, some of them include occludin and claudins [1, 2]. The mammalian nephron displays a wide spectrum of claudins, whose distribution varies in each tubular segment, thus determining the permeability properties of the renal epithelia. In the kidney, occludin is expressed along the nephron tubular segments [3, 4] and claudin-2 is expressed in leaky epithelia [5]. *In vitro* studies have shown that claudin-2 acts as a cation-selective paracellular pore [6] which mediates water transport in the renal proximal tubule [7]. E-cadherin is the major AJ protein expressed in epithelial cells and is highly expressed in the distal nephron and the collecting ducts, where it plays a role in decreasing paracellular permeability [8] and disruption of E-cadherin directly mediates epithelial-mesenchymal transition (EMT) downstream of transforming growth factor-beta1 (TGFβ1) in renal tubular epithelial cells [9]. Therefore, the TJ and AJ provide important adhesive contacts between neighboring epithelial cells. Previous studies have reported that TJ structure and function are sensitive to oxidative stress damage induced by several factors like heavy metals [10-12] and hydrogen peroxide (H_2O_2) [13]. Also, in early diabetic nephropathy, oxidative stress decreases occludin and claudin-2 expression in proximal tubules (PT) and claudin-5 in glomeruli (GL)[14].

Curcumin is a phenolic compound extracted from *Curcuma longa* rhizome and is used commonly in India, China and Southeast Asia as a spice, pigment, additive, and also in traditional medicine [15, 16]. Curcumin has broad biological functions, particularly antioxidant [17-21], anti-inflammatory [22], and renoprotective [17, 23-25]. Curcumin is a bifunctional antioxidant by the ability to exert both direct and indirect antioxidant effects [26]. It is able to react directly with reactive oxygen and nitrogen species [17] and induce the expression of several cytoprotective proteins [21, 26] many of them driven by nuclear factor erythroid-derived 2-like 2 (Nrf2) [27].

Cisplatin (CIS) is an effective anticancer drug used against lung and ovarian cancer and some lymphomas, however renal damage has limited its use [28-30]. Oxidative and nitrosative

stress are involved in the mechanism by which CIS induces renal damage [31, 32]. In this context it has been shown that curcumin administration provides protection against CIS-induced nephrotoxicity in rats [33, 34] and in mice [22]. Curcumin administration attenuates the CIS-induced decrease of antioxidant defense, including superoxide dismutase, catalase (CAT) and glutathione (GSH) [33]. Renal Nrf2 [35, 36] is decreased in CIS-induced nephrotoxicity and Nrf2 inductors are able to maintain its levels [35-38]. These findings suggest that Nrf2 regulation plays a role in CIS-induced nephrotoxicity and curcumin may induce Nrf2 in kidney [23, 24]. Rapid expression of the survival gene family heat shock protein 70 (Hsp70) was shown to be critical for mounting cytoprotection against severe cellular stress, as well as like elevated temperature (Hsp72) [39].

We previously reported that occludin and claudin-2 expressions are decreased in CIS-induced nephrotoxicity associated with oxidative stress derived in part to an increased production of superoxide anion ($O_2^{\bullet-}$) by nicotinamide adenine dinucleotide phosphate (NADPH) oxidase activity [32, 40]. The potential effect of curcumin against TGFβ1-induced EMT and fibrosis, and alterations in TJ and AJ structure and function has not been evaluated in CIS-induced nephrotoxicity. In this study was evaluated the potential protective effect of curcumin against renal fibrosis and alterations in TJ and AJ proteins. It was found that CIS induced renal damage, increase in profibrotic proteins such as TGFβ1, decrease in renal expression of occludin, claudin-2 and E-cadherin as well as oxidative/nitrosative stress evaluated by measuring malondialdehyde (MDA) levels, Hsp70/72 expression, 3-nitrotyrosine (3-NT) abundance, and expressions of Nrf2, NADPH oxidase subunits $p47^{phox}$ and $gp91^{phox}$ and protein kinase C (PKC) β2. All these changes were effectively prevented by curcumin pretreatment.

Experimental

Reagents and antibodies

Cis-diamineplatinum(II)dichloride [CIS, (Cat. No. 479306, Lt MKBH5984V)], curcumin [Cat. No. C1386, Lt 079K1756V], *2,2-azobis* (2-amidinopropane) dihydrochloride (AAPH), xanthine, xanthine oxidase, nitroblue tetrazolium (NBT), fluorescein, DL-penicillamine, diethylenetriaminepentaacetic acid (DTPA), *2,2*-diphenyl-1-picrylhydrazyl radical ($DPPH^{\cdot}$), terephtalic acid (TA), ascorbic acid, Amplex Red, horseradish peroxidase (HRP), sodium pyruvate, dimethylthiourea (DMTU), lipoic acid, GSH, glutathione disulfide (GSSG), *1*-chloro-*2,4*-dinitrobenzene (CDNB), nordihydroguaiaretic acid (NDGA), dimethyl sulfoxide (DMSO), phenylmethylsulfonyl fluoride (PMSF), sodium dodecyl sulfate (SDS), diphenylene iodonium (DPI), *1,3*-diphenylisobenzofuran (DPBF), *2,4,6*-Tris(2-pyridyl)-s-triazine (TPTZ), collagenase (from *Clostridium histolyticum*, type II), rabbit anti-PKCβ2 and rabbit anti-Nrf2 antibodies were from Sigma-Aldrich (St. Louis, MO, USA). Tiron (superoxide dismutase mimetic) was from Fluka (St. Louis, MO, USA). Dihydroethidium (DHE) was purchased form Molecular Probes (Eugene, OR, USA). Dihydrorhodamine 123 (DHR-123), *2′,7′*-dichlorofluorescein diacetate (DCDHF-DA) and mouse anti-3-NT antibody were from Cayman Chemical Co. (Ann Arbor, MI, USA). Trolox was from EMD Millipore (Billerica, MA, USA). Ethylenediaminetetraacetic acid (EDTA), sodium hypochlorite and H_2O_2 were from JT Baker (Xalostoc, Edo. Mexico, Mexico). The rabbit anti-claudin-2, rabbit anti-occludin, peroxidase-conjugated anti-rabbit, peroxidase-conjugated anti-mouse, peroxidase-conjugated anti-goat, Alexa Fluor® 488 donkey anti-rabbit, Alexa Fluor® 488 donkey anti-goat and Alexa Fluor® 594 donkey anti-mouse antibodies were purchased from Invitrogen (Carlsbad, CA, USA). Mouse anti-glyceraldehyde 3-phosphate dehydrogenase (GAPDH) antibody was purchased from Millipore Corp. (Billerica, MA, USA). Goat anti- kidney injury molecule-1 (KIM-1) was purchased from R&D Systems (McKinley Place, MN, USA). Mouse anti-Hsp70/72 antibody

was purchased from Enzo Life Sciences, Inc. (Farmingdale, NY, USA). The mouse anti-dipeptidylpeptidase (DppD)-IV antibody was purchased from AbD serotec (Raleigh, NC, USA). The mouse anti-desmoplakin (DMPK) 1/2 antibody was purchased from MP Biomedicals (Solon, OH, USA). The goat anti-$p47^{phox}$, goat anti-$gp91^{phox}$, rabbit anti-E-cadherin, rabbit anti- neutrophil gelatinase-associated lipocalin (NGAL), mouse anti-caspase-3, mouse anti-collagen I, mouse anti-collagen IV, mouse anti-α-alpha-smooth muscle actin (α-SMA), rabbit anti-β-catenin and rabbit anti-TGFβ1 antibodies were purchased from Santa Cruz Biotechnology, Inc. (Santa Cruz, CA, USA). Protease inhibitor cocktail Complete 1X (Roche Applied Science, Mannheim, Germany). Commercial kits for the measurement of blood urea nitrogen (BUN) and plasma creatinine concentration (Sera-pak plus creatinine Cat. No. 1001111 and urea Cat. No. 1001325) were from Spinreact (Girona, Spain). Micro BCA™ Protein Assay Reagent Kit was from Pierce (Rockford, IL, USA). All other reagents were of analytical grade and commercially available.

Ferric reducing ability power (FRAP) assay

The total antioxidant activity of curcumin was determined by FRAP assay (the ability to reduce Fe^{3+} to Fe^{2+}) as previously described [41].

In vitro reactive oxygen species (ROS) scavenging assays

In all scavenging assays solutions of curcumin at different concentrations (from a stock of 3 mg/ml in DMSO) were used and the optical densities or fluorescence units were obtained using a Synergy HT multimode microplate reader (Biotek Instruments, Winooski, VT, USA). In each assay a tube with water instead of curcumin or reference compound was used and considered as the 0% of scavenging activity. In addition, the scavenging activity of DMSO (as vehicle of curcumin) was tested in each assay.

Superoxide anion ($O_2^{\bullet-}$) scavenging assay

$O_2^{\bullet-}$ was generated by the xanthine-xanthine oxidase system. Scavenging activity of curcumin was determined by evaluating its ability to inhibit the $O_2^{\bullet-}$-induced DHR123 oxidation [42].

Singlet oxygen ($^1O_2$) scavenging assay

$^1O_2$ was generated from hypochlorite and H_2O_2 as previously described [43]. $^1O_2$ causes a reduction in fluorescence of DPBF that was determined at excitation and emission wavelengths of 410 nm and 455 nm, respectively.

H_2O_2 scavenging assay

The ability of curcumin to scavenge H_2O_2 was conducted using Amplex Red reagent. This compound is oxidized in the presence of H_2O_2 to produce resorufin, a fluorescent compound which is measured using excitation and emission filters of 530/25 and 590/35, respectively [43].

Hydroxyl radical ($OH^{\bullet}$) scavenging assay

$OH^{\bullet}$ was generated by the Fenton reaction [44]. Were obtain a fluorescent product that was detected at excitation and emission wavelengths of 326 nm and 432 nm, respectively.

Peroxynitrite anion ($ONOO^-$) scavenging assay

$ONOO^-$ was synthesized according to Cervantes et al [43]. DCDHF-DA was used as an indicator of the presence of this anion, in the absence of an antioxidant, DCDHF-DA is oxidized to dichlorofluorescein, a fluorescent compound that is measured at excitation and emission wavelengths of 502 and 523 nm, respectively.

Hypochlorous acid (HOCl) scavenging assay

The ability of curcumin to scavenge HOCl was determined using para-aminobenzoic acid which reacts with HOCl to produce the fluorescent compound 3-chloro-4-aminobenzoic acid [45]. The fluorescence was determined at excitation and emission wavelengths of 280 nm and 340 nm, respectively.

Peroxyl radical ($ROO^{\bullet}$) scavenging assay

The scavenging activity of curcumin was determined by the stability of the fluorescence of fluorescein by $ROO^{\bullet}$ [46]. Fluorescence was determined at excitation and emission wavelengths of 485 nm and 520 nm, respectively, for 1.5 h at 37°C. At the end of the assay the area under the curve was obtained by Gen 5 software (Biotek Instruments).

***In vivo* experimental model**

Twenty male Wistar rats (200-250 g) were fed with standard chow and water *ad libitum*. The animals were randomly distributed in 4 groups of 5 rats each: the first group received only vehicle (V, isotonic saline) by intraperitoneal injection (i.p.), the second group received a single i.p. dose of 5 mg/kg of CIS, a third group received three doses of curcumin by gavage (Cur+CIS, 200 mg/kg+5 mg/kg): 30 min before and 24 and 48 hours after CIS injection, and the fourth one received curcumin as described above. The doses of curcumin were based on previous studies [47] and the one of cisplatin was based on experiments (see Supplementary Figure 1). Seventy-two h after CIS administration, rats were anesthetized with sodium pentobarbital (90 mg/kg, i.p.); blood was collected from the aorta in heparinized tubes. Both kidneys were immediately dissected and frozen by immersion in liquid nitrogen. We followed the guidelines of the Official Mexican Standard Care and Use of Laboratory Animals (NOM-062-ZOO-1999) and the Local Ethics Committee (FQ/CICUAL/069/13) approved the protocol.

Determination of renal function

BUN, plasma creatinine, *N*-acetyl-β-D-glucosaminidase (NAG), NGAL, KIM-1 were used as markers of renal injury [32, 48]. BUN and plasma creatinine were determined with commercial kits from Spinreact® [49]. NAG activity was measured in kidney tissue by a colorimetric assay, as previously described [50]. KIM-1 was measured by Western blot and immunofluorescence and NGAL was measured by Western blot as described later.

Histological studies and apoptosis

Histological studies were performed as previously described [32]. H&E-stained paraffin section were assessed by an expert pathologist in a blind manner to experimental groups, with a digital camera incorporated to a Zeiss Axiophot 2 light microscope by means of an imaging software, AxioVision 4.8. The severity of tubular injury was calculated semi-quantitatively in eight random subcortical periglomerular fields (magnification x200) per each rat for cell detaching, apoptosis, acute tubular necrosis and cast formation, using a 0–scale: 0 (absence); 1+ (mild or <5%); 2+ (moderate or 5 to 25%); 3+ (severe or >25%) of juxtamedullary proximal tubules. Apoptosis was evaluated by analyzing the expression of cleaved caspase 3 by Western blot as described later.

Markers of oxidative stress

MDA, $O_2^{\bullet-}$ production in isolated GL and PT, 3-NT, expression of Hsp70/72, expression of PKCβ2, NADPH oxidase subunits $p47^{phox}$ and $gp91^{phox}$ and Nrf2 and activity of antioxidant enzymes were measured as markers of oxidative stress. Renal MDA concentration was measured as previously described [51]. The activities of antioxidants enzymes CAT and glutathione reductase (GR) were assayed in kidney homogenates as previously described [28].

Isolation of GL and PT

GL isolation was performed as previously described[14]. PT were isolated by Percoll gradients as previously described[14] and was confirmed by light microscopy observation.

$O_2^{\bullet-}$ production assay

Fluorescent detection of $O_2^{\bullet-}$ production in GL and PT was performed as described by Trujillo et al [40]. Fluorescence intensity of each sample was normalized relative to the control. Protein content was measured using the Lowry method.

Extraction of proteins from renal cortex for Western blot

Extraction of proteins from renal cortex was performed as described by Molina-Jijón et al [14]. Total protein quantification was performed using the Micro BCA Protein Assay Reagent Kit.

Western blot

Western blot analysis was performed as previously described [14]. Polyvinylidene difluoride (PVDF) membranes were incubated overnight at 4°C with the appropriate primary antibodies against NGAL, GAPDH, KIM-1, caspase-3, TGFβ1, collagen I, collagen IV, α-SMA, Nrf2, 3-NT, Hsp70/72, $p47^{phox}$, $gp91^{phox}$, PKCβ2, claudin-2, occludin and E-cadherin (used at a dilution 1:1,000). Peroxidase-conjugated anti-rabbit, anti-goat and anti-mouse were incubated for 1 h at room temperature (used at a dilution 1:20,000). Immunoblots were developed using the ECL™ prime Western blotting detection reagent (Amersham™, GE Healthcare, Buckinghamshire, UK). Chemiluminescence was detected in an EC3 Imaging System (UVP BioImaging Systems, Cambridge, UK). Protein band density was quantified by transmittance densitometry (ImageJ software, USA).

Immunofluorescence

Kidney samples were prepared for immunofluorescence as previously described [14]. Kidney sections were incubated overnight at 4°C with primary antibodies anti-KIM-1, anti-DppD, anti-claudin-2, anti-occludin, anti-E-cadherin (used at a dilution 1:100) and anti-DMPK (used at a dilution 1:50). DppD and DMPK were used as markers of proximal and distal tubules respectively. Secondary antibodies Alexa Fluor® 488 donkey anti-rabbit, Alexa Fluor® 488 donkey anti-goat and Alexa Fluor® 594 donkey anti-mouse were used at a 1:300 dilution. Immunofluorescence was evaluated using a confocal inverted microscope (TCS-SP8, Leica, Heidelberg, Germany). Immunofluorescence experiments were performed at least three times in samples from three different animals per group. Nonspecific labeling was estimated by omission of the primary antibodies.

Statistical analysis

All the values are expressed as mean ± standard error of the mean (SEM). Results of scavenging ability were expressed as IC_{50} (ability of the sample to scavenge 50% of each ROS). Values were determined by interpolation using the least squares method calculated from 3 independent experiments. One-way ANOVA and Bonferroni analysis were used to compare the in vivo data of the four groups, $p<0.05$ was considered significant.

Results and discussion

In vitro antioxidant activity of curcumin

Curcumin is a strong antioxidant compound and its renal protective effects have been studied in several models of renal oxidative damage[19, 22, 24, 25]. In order to demonstrate that the curcumin used in this study is functional we determined its antioxidant properties using several antioxidant assays such as FRAP method and ROS scavenging specific assays. The total antioxidant activity, measured by FRAP assay, showed that curcumin has the ability to reduce Fe^{3+} to Fe^{2+} and this capacity has a value of 4,548.2±109.4 μmoles of Fe_2SO_4 equivalents/g of curcumin. As shown in Figure 1, the specific antioxidant scavenging capacity of curcumin was tested for $O_2^{\bullet-}$, $^1O_2$, H_2O_2, $OH^{\bullet}$, $ONOO^-$, HOCl and $ROO^{\bullet}$, and compared with reference scavengers. IC_{50} values are summarized in Table 1. The order of curcumin IC_{50} values were the following: $HOCl>OH^{\bullet}>{}^1O_2>H_2O_2>O_2^{\bullet-}>ONOO^->ROO^{\bullet}$. Curcumin scavenges $ROO^{\bullet}$, $ONOO^-$, H_2O_2, and $^1O_2$, more efficiently than trolox, penicillamine, sodium pyruvate, and lipoic acid, respectively, since the IC_{50} value was smaller than the mentioned reference compounds (Table 1). The scavenging activity of curcumin for $OH^{\bullet}$ and HOCl was less efficient than their respective reference compounds, DMTU and ascorbic acid, respectively, meanwhile the scavenging activity of curcumin for $O_2^{\bullet-}$ was similar to Tiron. In addition, curcumin was able to scavenge these ROS in a concentration-dependent way (for

$ROO^{\bullet}$, 0.25-75 μg/ml, r^2=0.95315 ± 0.0059; for $ONOO^-$, 0.45-15 μg/ml, r^2=0.9489 ± 0.0279; for H_2O_2, 1-64 μg/ml, r^2=0.9734 ± 0.0069; for $^1O_2$, 1-125 μg/ml, r^2=0.9795 ± 0.0068; for $OH^{\bullet}$, 12.8-160 μg/ml, r^2=0.9669 ± 0.0056; for HOCl, 8-250 μg/ml, r^2=0.9853 ± 0.0047; for $O_2^{\bullet-}$, 1 to 64 μg /ml, r^2=0.9354 ± 0.0189). These data show that curcumin used in this work has efficient direct antioxidant properties.

***In vivo* experimental model**

Curcumin treatment improves renal function and KIM-1 expression in cisplatin-induced nephrotoxicity.

CIS is one of the most potent and effective anticancer drugs. However, its use is limited by its serious side effects such as nephrotoxicity, with proximal tubular epithelial cells as the primary target [52]. As shown, in supplementary Figure 1, CIS (5 mg/kg) significantly induced renal damage (evidenced by increased plasma creatinine, BUN, MDA and decreased CAT activity). It is known that CIS decreases the antioxidant status of the kidney by decreasing the expression of the transcription factor Nrf2 [36], consequently, leading to a failure of the antioxidant defense against ROS. We previously showed that CIS decreases the activity of the antioxidant enzymes CAT, glutathione peroxidase, and glutathione S-transferase in the kidney [49]. In previous studies, it has been reported that CIS induces the loss of the cell-cell contact of renal epithelial tubular cells, as well as apoptosis, by a mechanism dependent on PKC activation [32, 53].

Next, we analyzed the effect of curcumin on renal and tubular dysfunction and injury induced by CIS. As shown, curcumin significantly ameliorated the CIS-induced increment in plasma creatinine (Figure 2A), BUN (Figure 2B) and renal expression of NGAL (Figure 2D and E) and decrement of renal NAG (Figure 2C). Rats treated with curcumin alone showed similar values compared to control group. To evaluate tubular injury, KIM-1 (a sensitive marker of tubular

damage that is overexpressed when proximal tubules are found under proteinuric, toxic and ischemic kidney disease [54, 55]) expression was assessed by confocal microscopy (Figure 3A-D) and Western blot (Figure 3E and F) in kidneys from the four experimental groups. It was found that CIS increased KIM-1 expression in proximal tubules (label of KIM-1 co-localized with DppD, a marker of proximal tubular brush border) and that curcumin significantly decreased KIM-1. Curcumin group had similar labeling of KIM-1 to that of control group. In agreement with the functional results, KIM-1 expression increased in CIS treated rats and curcumin was able to attenuate this alteration. These data suggest that curcumin treatment exerted renoprotective effect on CIS-induced renal damage. However, Namboothiri et al., (2008) [56] patented that hydrazino derivatives of curcumin possess an enhanced stability and process for preparation thereof with highly potent chemotherapeutic actions, raising the possibility that these compounds may be better for the treatment of CIS nephrotoxicity.

Curcumin prevents acute tubular necrosis and apoptosis induced by cisplatin.

It has been widely described that in CIS-induced nephrotoxicity, histopathological abnormalities are developed, such as: apoptosis, acute tubular necrosis, degeneration and desquamation, karyomegaly, tubular dilatation, interstitial mononuclear cell infiltration and cast formation in the tubular lumen [32, 57, 58]. Cisplatin-induced acute tubular necrosis and apoptosis are associated with the formation of platinum-DNA adducts, which are formed after the uptake of the drug into the nucleus of cells, where activates several cellular processes that mediates the cytotoxicity, including those involved in regulating drug uptake, the signaling of DNA damage, cell-cycle checkpoints and arrest cellular, DNA repair and cell death [59]. On the other hand it has been reported that curcumin together with cisplatin may result synergism in the generation of platinum-DNA adducts; however these studies have only been carried out in cultured cancer cell lines [60] . Curcumin ameliorates histological changes in CIS-induced

nephrotoxicity [22, 33]. In this study, to corroborate that curcumin prevents the development of histopathological alterations, H&E staining was performed (Figure 4A-D). It was found that curcumin-treated rats showed minor characteristic alterations in renal tissue after acute injury induced by CIS, such lesser cell detaching, apoptosis, tubular necrosis and cast formation in the tubular lumen (Figure 4C; Table 2). However curcumin was unable to prevent 100% the histological damage induced by CIS. Interestingly, this has been observed in another model of renal damage induced by maleate [61]. We are tempting to speculate that a higher dose of curcumin may be needed to prevent 100% the histological damage in this experimental model. To evaluate cell death by apoptosis, Western blot of caspase 3 was performed in renal tissue (Figure 4E and F). As shown, curcumin decreased the increment of cleaved-caspase 3 (Figure 4E, band of 17 KDa) induced by CIS. This is in agreement with previous studies where the anti-apoptotic mechanism exerted by curcumin is associated with its ability to inhibit TGF-β signaling [62] and to induce Bcl2 expression [63]. However, no changes were found in pro-caspase 3 expression in the four experimental groups studied (Figure 4E, band of 35 KDa). Densitometric analysis of cleaved-caspase 3/pro-caspase 3 ratio is shown in figure 4F. These data suggest that curcumin exerts antiapoptotic effect in CIS-induced renal injury.

Curcumin prevents cisplatin-induced renal fibrosis.

Several studies have demonstrated that many mechanisms, including oxidative stress, DNA damage, inflammatory responses and fibrosis, are closely associated with CIS-induced nephrotoxicity. The effect of curcumin on CIS-induced testicular fibrosis has been previously explored [64]. CIS is reported to induce tubule interstitial fibrosis as early as 2 weeks post-exposure [65]. However, to our knowledge, the effect of curcumin on short-term renal fibrosis induced by CIS has not been described. In order to study whether fibrosis is involved in CIS-induced nephrotoxicity, the profibrotic proteins TGFβ1, collagens-I and –IV, and α-SMA were

evaluated by Western blot in renal cortex homogenates from the four experimental groups studied. Figure 5 shows that curcumin decreased the expression of TGFβ1 (Figure 5A and E), collagens-I and –IV (Figure 5B, C and E), and α-SMA (Figure 5D and E) induced by CIS. These findings suggest that curcumin decreased structural alterations associated with fibrosis.

Curcumin prevents cisplatin-induced oxidative stress.

We have previously described that oxidative stress contributes to renal damage induced by CIS and curcumin induces the activity of antioxidant enzymes such as superoxide dismutase and glutathione peroxidase by maintaining or inducing Nrf2 expression [20, 23]. Also, curcumin protects against the H_2O_2-induced intestinal barrier disruption by inducing the expression of the antioxidant enzyme heme oxygenase (HO)-1[66]. To assess this issue, MDA levels, activity of CAT and GR, Hsp70/72, Nrf2 and 3-NT expressions were measured in the four experimental groups studied. As shown in Figure 6, curcumin ameliorated CIS-induced increase in MDA levels (Figure 6A), Hsp70/72 (Figure 6D and G) and 3-NT expression (Figure 6F and G) and also the decrease in the activity of antioxidant enzymes such as CAT (Figure 6B) and GR (Figure 6C) and Nrf2 expression (Figure 6E and G). No changes were found in the group treated with curcumin alone compared to the control group. Sahin et al [67] reported that curcumin reduces thermal stress through modulation of the expression of Hsp70, Nrf2 and HO-1. Protein tyrosine nitration is a posttranslational modification induced by $ONOO^-$ under oxidative stress conditions and increased nitration of proteins modifies the structure and function of the target protein [68]. CIS induced 3-NT and curcumin treatment was able to attenuate the increment in 3-NT. These findings strongly suggest that its antioxidant effects, maintaining Nrf2 levels and decreasing protein tyrosine nitration, mediate the nephroprotection exerted by curcumin.

Curcumin ameliorates the increment of $O_2^{\bullet-}$ production in GL and PT and expression of NADPH oxidase $p47^{phox}$ and $gp91^{phox}$ subunits and PKCβ2 induced by cisplatin.

We previously reported that CIS induces $O_2^{\bullet-}$ production in GL and PT and to a lesser extent in distal tubules by a mechanism dependent on NADPH oxidase activity [40]. In order to evaluate the effect of curcumin on increased NADPH oxidase activity induced by CIS, $O_2^{\bullet-}$ production was evaluated by using NADH as substrate and DPI as inhibitor, on freshly isolated GL and PT from the four experimental groups. It was found that curcumin decreased CIS induced increment of $O_2^{\bullet-}$ production in GL (Figure 7A) and PT (Figure 7B). $O_2^{\bullet-}$ production in samples obtained from CIS group was decreased by DPI treatment, suggesting that NADPH oxidase is the source of this ROS. Also, NADPH oxidase $p47^{phox}$ and $gp91^{phox}$ subunits were assessed. It was found that curcumin decreases the increment of $p47^{phox}$ (Figure 7C and F) and $gp91^{phox}$ (Figure 7D and F) subunits induced by CIS, thus suggesting the association between the decreased expression of $p47^{phox}$ and $gp91^{phox}$ with the decreased $O_2^{\bullet-}$ production in the CIS+Cur group. No changes were found in the curcumin alone treated group compared to V group. It has been reported that PKC-related signal transduction pathways might modulate CIS nephrotoxicity [69]. Also, we have previously reported that CIS increased expression of $p47^{phox}$ and $gp91^{phox}$ subunits by a PKCβ2-dependent way, which might promote the assembly of NADPH oxidase active complex [69, 70]. Herein $PKC\beta_2$ expression was analyzed in the four experimental groups studied, Figures 7E and F show that CIS significantly induced PKCβ2 expression in renal cortex. Curcumin pretreatment decreased CIS-induced increase in PKCβ2 expression (Figure 7E and F). This finding suggests that curcumin nephroprotection may be related to NADPH oxidase activity, $p47^{phox}$ and $gp91^{phox}$ subunits and PKCβ2 inhibition in GL and PT.

Curcumin treatment prevents loss of renal tight junction proteins claudin-2 and occludin and adherens junction E-cadherin and β-catenin induced by cisplatin.

It has been described that CIS causes the loss of cell-cell contacts of renal proximal tubular epithelial cells by altering the localization of the AJ-associated protein β-catenin [53] leading to apoptosis of the proximal tubular cells. In this study, it was explored whether renal TJ and AJ are altered in CIS-induced nephrotoxicity. We next analyze whether CIS affects the distribution and expression levels of renal TJ proteins claudin-2 and occludin and AJ proteins E-cadherin and β-catenin; claudin-2 is located at the PT [5] and occludin and E-cadherin which are expressed mainly in the distal segments [8, 71, 72]. Confocal microscopy and Western blot analyses were performed to evaluate the distribution and expression levels of TJ and AJ proteins, respectively. Western blot of claudin-2, occludin, E-cadherin and β-catenin, in renal cortex homogenates were performed in the four experimental groups studied. The expressions of claudin-2 (Figures 8A-D), occludin (Figures 8E-H), E-cadherin (Figure 9A-D) and β-catenin (Figure 9F) were decreased in CIS-treated rats, as shown by immunofluorescence and Western blot (Figures 8I and J and Figure 9E). Under control conditions (V- and curcumin-treated groups), it can be observed the localization of occludin and claudin-2 and E-cadherin as a typical chicken fence pattern in cell borders of proximal and distal tubules, respectively. In contrast, in the CIS-treated group, the localization of occludin, claudin-2 and E-cadherin in cell borders was discontinuous and almost disappears. This is important, as claudin-2 is needed for the tubular reabsorption of sodium and the maintenance of cell-cell contacts of the proximal tubular cells [5]. These findings suggest that claudin-2 absence or decreased expression induced by CIS might be linked to tubular dysfunction. Also, increased activity of conventional PKC isoforms, such as PKCβ, is involved in the phosphorylation of TJs components. In general, conventional PKC isoforms participate

in the disassembly of the TJ [72] suggesting that the activation of PKCβ2 induced by CIS might explain the loss of claudin-2 and occludin in the PT. Additionally, it has been reported that PKCβ2 co-immunoprecipitates with claudin-2 and promotes its serine phosphorylation in early diabetic nephropathy, this change was associated with decreased expression of claudin-2 [73]. Curcumin treatment was able to significantly prevent the loss of claudin-2 (Figure 8C and I) and occludin (Figure 8G and J) induced by CIS. DppD, a marker of PT, did not change, indicating that the decrements in claudin-2 and occludin expressions were selective. E-cadherin, the major component of AJ that decreases the paracellular permeability of the distal nephron [8] was decreased by CIS and also, curcumin prevented loss of the AJ-associated protein E-cadherin induced by CIS (Figure 9C and 9E). It has been described that PKC mediates cisplatin-induced delocalization of β-catenin in LLC-PK1 cells [53], herein we found that cisplatin increases PKCβ2 and decreases β-catenin expressions, thus suggesting that PKCβ2 might mediate loss of β-catenin induced by cisplatin and that curcumin prevented loss of β-catenin by decreasing PKCβ2.

Together with TGFβ is known as one of strong profibrogenic factors that mediates EMT [74, 75], in this process epithelial markers such as E-cadherin and claudins are lost whilst increased expression of collagens and α-SMA are favored. Based on the findings described above it can be concluded that curcumin decreases CIS-induced EMT and fibrosis Thus, curcumin treatment was able to prevent CIS-induced mislocalization of TJ and AJ proteins from cell borders [66]. In conclusion, these data suggests that curcumin treatment prevents loss of cell-cell contacts induced by CIS.

Conclusions

In conclusion, we propose that the pathway through which curcumin ameliorates CIS-induced EMT and fibrosis and decreased expression of the tight (claudin-2 and occludin) and adherens (E-cadherin) junction proteins might be linked to its antioxidant properties. A scheme showing the mechanism proposed in this study is shown in Figure 10.

Acnowledgements

CONACYT (Grants 220046 and 252008) and PAPIIT No. IN210713 supported this work.

References

1. M. Furuse, T. Hirase, M. Itoh, A. Nagafuchi, S. Yonemura, S. Tsukita and S. Tsukita, *The Journal of cell biology*, 1993, **123**, 1777-1788.
2. M. Furuse, K. Fujita, T. Hiiragi, K. Fujimoto and S. Tsukita, *The Journal of cell biology*, 1998, **141**, 1539-1550.
3. O. Kwon, B. D. Myers, R. Sibley, D. Dafoe, E. Alfrey and W. J. Nelson, *The journal of histochemistry and cytochemistry : official journal of the Histochemistry Society*, 1998, **46**, 1423-1434.
4. J. L. Reyes, M. Lamas, D. Martin, M. del Carmen Namorado, S. Islas, J. Luna, M. Tauc and L. Gonzalez-Mariscal, *Kidney international*, 2002, **62**, 476-487.
5. A. H. Enck, U. V. Berger and A. S. Yu, *American journal of physiology. Renal physiology*, 2001, **281**, F966-974.
6. Y. Kiuchi-Saishin, S. Gotoh, M. Furuse, A. Takasuga, Y. Tano and S. Tsukita, *Journal of the American Society of Nephrology : JASN*, 2002, **13**, 875-886.
7. R. Rosenthal, S. Milatz, S. M. Krug, B. Oelrich, J. D. Schulzke, S. Amasheh, D. Gunzel and M. Fromm, *Journal of cell science*, 2010, **123**, 1913-1921.
8. A. O. Perantoni, *Experimental nephrology*, 1999, **7**, 80-102.
9. G. Zheng, J. G. Lyons, T. K. Tan, Y. Wang, T. T. Hsu, D. Min, L. Succar, G. K. Rangan, M. Hu, B. R. Henderson, S. I. Alexander and D. C. Harris, *The American journal of pathology*, 2009, **175**, 580-591.
10. W. C. Prozialeck and R. J. Niewenhuis, *Toxicology and applied pharmacology*, 1991, **107**, 81-97.
11. G. Jacquillet, O. Barbier, M. Cougnon, M. Tauc, M. C. Namorado, D. Martin, J. L. Reyes and P. Poujeol, *American journal of physiology. Renal physiology*, 2006, **290**, F127-137.
12. L. Arreola-Mendoza, L. M. Del Razo, M. E. Mendoza-Garrido, D. Martin, M. C. Namorado, J. V. Calderon-Salinas and J. L. Reyes, *Toxicology letters*, 2009, **191**, 279-288.
13. T. N. Meyer, C. Schwesinger, J. Ye, B. M. Denker and S. K. Nigam, *The Journal of biological chemistry*, 2001, **276**, 22048-22055.
14. E. Molina-Jijon, R. Rodriguez-Munoz, C. Namorado Mdel, J. Pedraza-Chaverri and J. L. Reyes, *Free radical biology & medicine*, 2014, **72**, 162-175.
15. T. Esatbeyoglu, P. Huebbe, I. M. Ernst, D. Chin, A. E. Wagner and G. Rimbach, *Angewandte Chemie*, 2012, **51**, 5308-5332.

16. A. Goel, A. B. Kunnumakkara and B. B. Aggarwal, *Biochemical pharmacology*, 2008, **75**, 787-809.
17. T. Osawa, *Advances in experimental medicine and biology*, 2007, **595**, 407-423.
18. A. Gonzalez-Salazar, E. Molina-Jijon, F. Correa, G. Zarco-Marquez, M. Calderon-Oliver, E. Tapia, C. Zazueta and J. Pedraza-Chaverri, *Cardiovascular toxicology*, 2011, **11**, 357-364.
19. F. Correa, M. Buelna-Chontal, S. Hernandez-Resendiz, R. G.-N. W, J. R. F, V. Soto, A. Silva-Palacios, A. Amador, J. Pedraza-Chaverri, E. Tapia and C. Zazueta, *Free radical biology & medicine*, 2013, **61**, 119-129.
20. I. Carmona-Ramirez, A. Santamaria, J. C. Tobon-Velasco, M. Orozco-Ibarra, I. G. Gonzalez-Herrera, J. Pedraza-Chaverri and P. D. Maldonado, *The Journal of nutritional biochemistry*, 2013, **24**, 14-24.
21. L. M. Reyes-Fermin, S. Gonzalez-Reyes, N. G. Tarco-Alvarez, M. Hernandez-Nava, M. Orozco-Ibarra and J. Pedraza-Chaverri, *Nutritional neuroscience*, 2012, **15**, 34-41.
22. M. Ueki, M. Ueno, J. Morishita and N. Maekawa, *Journal of bioscience and bioengineering*, 2013, **115**, 547-551.
23. E. Tapia, V. Soto, K. M. Ortiz-Vega, G. Zarco-Marquez, E. Molina-Jijon, M. Cristobal-Garcia, J. Santamaria, W. R. Garcia-Nino, F. Correa, C. Zazueta and J. Pedraza-Chaverri, *Oxidative medicine and cellular longevity*, 2012, **2012**, 269039.
24. E. Tapia, Z. L. Zatarain-Barron, R. Hernandez-Pando, G. Zarco-Marquez, E. Molina-Jijon, M. Cristobal-Garcia, J. Santamaria and J. Pedraza-Chaverri, *Phytomedicine : international journal of phytotherapy and phytopharmacology*, 2013, **20**, 359-366.
25. E. Molina-Jijon, E. Tapia, C. Zazueta, M. El Hafidi, Z. L. Zatarain-Barron, R. Hernandez-Pando, O. N. Medina-Campos, G. Zarco-Marquez, I. Torres and J. Pedraza-Chaverri, *Free radical biology & medicine*, 2011, **51**, 1543-1557.
26. A. T. Dinkova-Kostova and P. Talalay, *Molecular nutrition & food research*, 2008, **52 Suppl 1**, S128-138.
27. V. Calabrese, T. E. Bates, C. Mancuso, C. Cornelius, B. Ventimiglia, M. T. Cambria, L. Di Renzo, A. De Lorenzo and A. T. Dinkova-Kostova, *Molecular nutrition & food research*, 2008, **52**, 1062-1073.
28. J. M. Perez-Rojas, C. Cruz, P. Garcia-Lopez, D. J. Sanchez-Gonzalez, C. M. Martinez-Martinez, G. Ceballos, M. Espinosa, J. Melendez-Zajgla and J. Pedraza-Chaverri, *Free radical research*, 2009, **43**, 1122-1132.
29. J. M. Perez-Rojas, C. E. Guerrero-Beltran, C. Cruz, D. J. Sanchez-Gonzalez, C. M. Martinez-Martinez and J. Pedraza-Chaverri, *Food and chemical toxicology : an international journal published for the British Industrial Biological Research Association*, 2011, **49**, 2631-2637.
30. C. E. Guerrero-Beltran, P. Mukhopadhyay, B. Horvath, M. Rajesh, E. Tapia, I. Garcia-Torres, J. Pedraza-Chaverri and P. Pacher, *The Journal of nutritional biochemistry*, 2012, **23**, 494-500.
31. Y. I. Chirino and J. Pedraza-Chaverri, *Experimental and toxicologic pathology : official journal of the Gesellschaft fur Toxikologische Pathologie*, 2009, **61**, 223-242.
32. J. Trujillo, E. Molina-Jijon, O. N. Medina-Campos, R. Rodriguez-Munoz, J. L. Reyes, M. L. Loredo, E. Tapia, L. G. Sanchez-Lozada, D. Barrera-Oviedo and J. Pedraza-Chaverri, *Toxicology mechanisms and methods*, 2014, **24**, 520-528.
33. A. Kuhad, S. Pilkhwal, S. Sharma, N. Tirkey and K. Chopra, *Journal of agricultural and food chemistry*, 2007, **55**, 10150-10155.
34. S. Ugur, R. Ulu, A. Dogukan, A. Gurel, I. P. Yigit, N. Gozel, B. Aygen and N. Ilhan, *Renal failure*, 2015, **37**, 332-336.

35. K. Sahin, M. Tuzcu, H. Gencoglu, A. Dogukan, M. Timurkan, N. Sahin, A. Aslan and O. Kucuk, *Life sciences*, 2010, **87**, 240-245.
36. K. Sahin, M. Tuzcu, N. Sahin, S. Ali and O. Kucuk, *Food and chemical toxicology : an international journal published for the British Industrial Biological Research Association*, 2010, **48**, 2670-2674.
37. L. M. Aleksunes, M. J. Goedken, C. E. Rockwell, J. Thomale, J. E. Manautou and C. D. Klaassen, *The Journal of pharmacology and experimental therapeutics*, 2010, **335**, 2-12.
38. U. Kilic, E. Kilic, Z. Tuzcu, M. Tuzcu, I. H. Ozercan, O. Yilmaz, F. Sahin and K. Sahin, *Nutrition & metabolism*, 2013, **10**, 7.
39. G. Briassoulis, E. Briassouli, D. M. Fitrolaki, I. Plati, K. Apostolou, T. Tavladaki and A. M. Spanaki, *BioMed research international*, 2014, **2014**, 101023.
40. J. Trujillo, E. Molina-Jijon, O. N. Medina-Campos, R. Rodriguez-Munoz, J. L. Reyes, D. Barrera and J. Pedraza-Chaverri, *Journal of biochemical and molecular toxicology*, 2015, **29**, 149-156.
41. I. F. Benzie and J. J. Strain, *Analytical biochemistry*, 1996, **239**, 70-76.
42. S. Yanagisawa, A. Koarai, H. Sugiura, T. Ichikawa, M. Kanda, R. Tanaka, K. Akamatsu, T. Hirano, K. Matsunaga, Y. Minakata and M. Ichinose, *Respiratory research*, 2009, **10**, 50.
43. M. I. Cervantes, P. M. de Oca Balderas, J. de Jesus Gutierrez-Banos, M. Orozco-Ibarra, B. Fernandez-Rojas, O. N. Medina-Campos, M. Espinoza-Rojo, M. Ruiz-Tachiquin, A. Ortiz-Plata, M. I. Salazar, M. Rubio-Osornio, E. Castaneda-Saucedo, J. Pedraza-Chaverri, F. Calzada and P. Aguilera, *Food chemistry*, 2013, **140**, 343-352.
44. L. Gaona-Gaona, E. Molina-Jijon, E. Tapia, C. Zazueta, R. Hernandez-Pando, M. Calderon-Oliver, G. Zarco-Marquez, E. Pinzon and J. Pedraza-Chaverri, *Toxicology*, 2011, **286**, 20-27.
45. P. Van Antwerpen and J. Neve, *European journal of pharmacology*, 2004, **496**, 55-61.
46. D. Huang, B. Ou, M. Hampsch-Woodill, J. A. Flanagan and R. L. Prior, *Journal of agricultural and food chemistry*, 2002, **50**, 4437-4444.
47. M. Waseem, P. Kaushik and S. Parvez, *Cell biochemistry and function*, 2013, **31**, 678-684.
48. N. Srisawat, R. Murugan and J. A. Kellum, *Nephron. Clinical practice*, 2014, **127**, 185-189.
49. C. E. Guerrero-Beltran, M. Calderon-Oliver, E. Tapia, O. N. Medina-Campos, D. J. Sanchez-Gonzalez, C. M. Martinez-Martinez, K. M. Ortiz-Vega, M. Franco and J. Pedraza-Chaverri, *Toxicology letters*, 2010, **192**, 278-285.
50. Y. I. Chirino, R. Hernandez-Pando and J. Pedraza-Chaverri, *BMC pharmacology*, 2004, **4**, 20.
51. A. S. Jimenez-Osorio, A. Picazo, S. Gonzalez-Reyes, D. Barrera-Oviedo, M. E. Rodriguez-Arellano and J. Pedraza-Chaverri, *International journal of molecular sciences*, 2014, **15**, 20290-20305.
52. R. P. Miller, R. K. Tadagavadi, G. Ramesh and W. B. Reeves, *Toxins*, 2010, **2**, 2490-2518.
53. R. Imamdi, M. de Graauw and B. van de Water, *The Journal of pharmacology and experimental therapeutics*, 2004, **311**, 892-903.
54. A. B. Kramer, M. M. van Timmeren, T. A. Schuurs, V. S. Vaidya, J. V. Bonventre, H. van Goor and G. Navis, *American journal of physiology. Renal physiology*, 2009, **296**, F1136-1145.
55. J. V. Bonventre, *Nephrology, dialysis, transplantation : official publication of the European Dialysis and Transplant Association - European Renal Association*, 2009, **24**, 3265-3268.
56. *Bombay. Pat.,* 254150, 2008. US Pat., SN, 2012
57. A. Atessahin, A. O. Ceribasi, A. Yuce, O. Bulmus and G. Cikim, *Basic & clinical pharmacology & toxicology*, 2007, **100**, 121-126.
58. B. Rasoulian, M. Jafari, M. Mahbod, M. E. Dehaj, M. Nowrozi, H. Wahhabaghai, M. Mofid, A. Ghasemi, M. R. Bigdeli and A. Khoshbaten, *Renal failure*, 2010, **32**, 234-242.

59. A. J. Danford, D. Wang, Q. Wang, T. D. Tullius and S. J. Lippard, *Proceedings of the National Academy of Sciences of the United States of America*, 2005, **102**, 12311-12316.
60. N. M. Yunos, P. Beale, J. Q. Yu and F. Huq, *Anticancer Research*, 2011, **31**, 4283-4289.
61. E. Tapia, L. G. Sanchez-Lozada, W. R. Garcia-Nino, E. Garcia, A. Cerecedo, F. E. Garcia-Arroyo, H. Osorio, A. Arellano, M. Cristobal-Garcia, M. L. Loredo, E. Molina-Jijon, J. Hernandez-Damian, M. Negrette-Guzman, C. Zazueta, S. Huerta-Yepez, J. L. Reyes, M. Madero and J. Pedraza-Chaverri, *Free radical research*, 2014, **48**, 1342-1354.
62. A. S. Awad and A. A. El-Sharif, *Int Immunopharmacol*, 2011, **11**, 992-996.
63. A. M. El-Mahalaway, *Int J Clin Exp Pathol*, 2015, **8**, 6019-6030.
64. Y. O. Ilbey, E. Ozbek, M. Cekmen, A. Simsek, A. Otunctemur and A. Somay, *Human reproduction*, 2009, **24**, 1717-1725.
65. Y. Kawai, T. Satoh, D. Hibi, Y. Ohno, Y. Kohda, K. Miura and M. Gemba, *Journal of pharmacological sciences*, 2009, **111**, 433-439.
66. N. Wang, G. Wang, J. Hao, J. Ma, Y. Wang, X. Jiang and H. Jiang, *Digestive diseases and sciences*, 2012, **57**, 1792-1801.
67. K. Sahin, C. Orhan, Z. Tuzcu, M. Tuzcu and N. Sahin, *Food and chemical toxicology : an international journal published for the British Industrial Biological Research Association*, 2012, **50**, 4035-4041.
68. R. Radi, *Accounts of chemical research*, 2013, **46**, 550-559.
69. S. Ikeda, A. Fukuzaki, H. Kaneto, S. Ishidoya and S. Orikasa, *International journal of urology : official journal of the Japanese Urological Association*, 1999, **6**, 245-250.
70. T. Gomez-Sierra, E. Molina-Jijon, E. Tapia, R. Hernandez-Pando, W. R. Garcia-Nino, P. D. Maldonado, J. L. Reyes, D. Barrera-Oviedo, I. Torres and J. Pedraza-Chaverri, *The Journal of pharmacy and pharmacology*, 2014, **66**, 1271-1281.
71. L. Gonzalez-Mariscal, M. C. Namorado, D. Martin, J. Luna, L. Alarcon, S. Islas, L. Valencia, P. Muriel, L. Ponce and J. L. Reyes, *Kidney international*, 2000, **57**, 2386-2402.
72. L. Gonzalez-Mariscal, R. Tapia and D. Chamorro, *Biochimica et biophysica acta*, 2008, **1778**, 729-756.
73. E. Molina-Jijon, R. Rodriguez-Munoz, C. Namorado Mdel, P. Bautista-Garcia, O. N. Medina-Campos, J. Pedraza-Chaverri and J. L. Reyes, *The Journal of nutritional biochemistry*, 2015, **26**, 441-454.
74. T. A. Wynn, *The Journal of pathology*, 2008, **214**, 199-210.
75. D. Pohlers, J. Brenmoehl, I. Loffler, C. K. Muller, C. Leipner, S. Schultze-Mosgau, A. Stallmach, R. W. Kinne and G. Wolf, *Biochimica et biophysica acta*, 2009, **1792**, 746-756.

Figure legends

Figure 1. Curcumin scavenging activity. **A:** superoxide anion ($O_2^{\bullet -}$), **B:** singlet oxygen ($^1O_2$), **C:** hydrogen peroxide (H_2O_2), **D:** hydroxyl radical ($OH^{\bullet}$), **E:** peroxynitrite anion ($ONOO^-$), **F:** hypochlorous acid (HOCl), **G:** peroxyl radical ($ROO^{\bullet}$). In all scavenging assays, solutions of curcumin at different concentrations (0.25-250 μg/ml) were used; percentage of scavenging activity is shown. Data are shown as mean±SEM; n=3.

Figure 2. Renal injury markers in rats treated with vehicle (V, n=5), 5 mg/kg of cisplatin (CIS, n=9), 5 mg/kg of cisplatin + 200 mg/kg of curcumin (CIS+Cur, n=9) and 200 mg/kg of curcumin alone (Cur, n=5). (A) Plasma creatinine, (B) blood urea nitrogen (BUN), (C)N-acetyl-β-D-glucosaminidase (NAG), (D) neutrophil gelatinase-associated lipocalin (NGAL) is shown. A representative image of NGAL Western blot is shown in panel E. Data are expressed as relative density from 3 rats/group normalized with glyceraldehyde 3 phosphate dehydrogenase (GADPH) as loading control. Values are means±SEM. *P<0.05 vs. V; † p<0.05 vs. CIS.

Figure 3. Kidney injury molecule-1 (KIM-1) expression was evaluated by confocal microscopy (panels A-D, green label). Representative photomicrographs of kidney layers obtained from rats treated with: vehicle group (V; panel A), 5 mg/kg of cisplatin (CIS, panel B), 5 mg/kg of cisplatin + 200 mg/kg of curcumin (CIS+Cur, panel C) and 200 mg/kg of curcumin (Cur, panel D). The expression of dipeptidyl peptidase (DppD; red label) was used as a marker of the proximal tubule apical membrane and 4', 6-diamine-2-phenylindole (DAPI; blue label) was used as a marker of the nuclei. Merge images are shown in major panels A-D. Representative

Western blot for KIM-1 is shown in panel E and densitometric analyses of Western blots are shown in panel F; data are expressed as relative density from 3 rats/group normalized with glyceraldehyde-3-phosphate dehydrogenase (GAPDH) as loading control. Values are means±SEM. *P<0.05 vs. V; † p<0.05 vs. CIS. Bar=50 μm.

Figure 4. Representative renal light microscopy of kidney layers obtained form rats treated with (A) vehicle (V) and (B) 5 mg/kg of cisplatin (CIS). Apoptotic cells (↑), acute tubular necrosis (*) and formation of tubular casts (★) in the corticomedullary junction are shown. Additional groups of rats were treated with (C) 5 mg/kg of cisplatin + 200 mg/kg of curcumin (CIS+Cur) and (D) 200 mg/kg of curcumin (Cur). Kidney slides were stained with H&E-staining, original magnification 200x. Expression of cleaved-caspase 3 in kidney homogenates, representative western blots of pro-caspase 3 and cleaved-caspase 3 is shown in panel E, and densitometric analysis of Western blots is shown in panel F. Data are expressed as the ratio cleaved-caspase 3/pro-caspase 3 of 3 rats/group, both bands were corrected with glyceraldehyde-3-phosphate dehydrogenase (GAPDH) as loading control. Values are means±SEM. *P<0.05 vs. V; † p<0.05 vs. CIS. Bar=50 μm.

Figure 5. Proteins profibrotic factors were assessed by Western blot analysis in kidney homogenates of rats treated with vehicle (V), 5 mg/kg of cisplatin (CIS), 5 mg/kg of cisplatin + 200 mg/kg of curcumin (CIS+Cur) and 200 mg/kg of curcumin (Cur). Expression of transforming growth factor beta 1 (TGFβ1; panels A and E), collagen I (B and E), collagen IV (C and E) and alpha-smooth muscle actin (α-SMA; D and E) is shown. Representative Western blots of TGFβ1, collagen I, collagen IV, α–SMA and glyceraldehyde-3-phosphate dehydrogenase (GAPDH) are shown in panel E. Data are expressed as relative density from

3 rats/group normalized with GAPDH as a loading control, GAPDH is shown for every protein. Values are means ± SEM. *P<0.05 vs. V; † p<0.05 vs. CIS.

Figure 6. (A) Malondialdehyde (MDA) levels, activity of antioxidant enzymes: (B) catalase (CAT) and (C) glutathione reductase (GR), (D) family heat shock protein 70 (Hsp70/72), (E) nuclear factor erythroid-derived 2-like 2 (Nrf2), (F) expression and protein tyrosine nitration (3-NT) in renal tissue of rats treated with vehicle (V), 5 mg/kg of cisplatin (CIS), 5 mg/kg of cisplatin + 200 mg/kg of curcumin (CIS+Cur) and 200 mg/kg of curcumin (Cur). A representative Western blot images of Hsp70/72, Nrf-2, 3-NT and GADPH are shown in panel G. Data are expressed as relative density from 3 rats/group normalized with GADPH as loading control. Values are means±SEM. *P<0.05 vs. V; † p<0.05 vs. CIS.

Figure 7. Superoxide anion ($O_2^{\bullet -}$) production in (A) isolated glomeruli and (B) proximal tubules and renal expression of NADPH oxidase subunits (C) $p47^{phox}$ and (D) $gp91^{phox}$ and (E) protein kinase C (PKC) β2 of rats treated with vehicle (V), 5 mg/kg of cisplatin (CIS), 5 mg/kg of cisplatin + 200 mg/kg of curcumin (CIS+Cur) and 200 mg/kg of curcumin (Cur). $O_2^{\bullet -}$ production in samples from CIS-treated rats was also evaluated in the presence of the inhibitor of the NADPH oxidase, diphenylene iodonium (DPI; bar with diagonal lines). Data are expressed as $O_2^{\bullet -}$ production (/control), n=5 rats per group. A representative Western blot image of NADPH oxidase subunits $p47^{phox}$ and $gp91^{phox}$, PKCβ2 and GADPH are shown in panel F. Data are expressed as relative density from 3 rats/group normalized with glyceraldehyde-3-phosphate dehydrogenase (GAPDH) as a loading control each. Values are means±SEM. *P<0.05 vs. V; † p<0.05 vs. CIS.

Figure 8. Immunofluorescence of kidney layers obtained from rats treated with vehicle (V, panels A and E), 5 mg/kg of cisplatin (CIS, panels B and F), 5 mg/kg of cisplatin + 200 mg/kg of curcumin (CIS+Cur, panels C and G) and 200 mg/kg of curcumin (Cur, panels D and H) of claudin-2 (panels A-D; green label) and occludin (panels E-H; green label), both proteins were detected surrounding the brush border of proximal tubular cells. Dipeptidyl peptidase (DppD; red label) was used as a marker of the proximal tubule apical membrane and 4', 6-diamine-2-phenylindole (DAPI; blue label) was used to mark nuclei. Merge image of markers is shown in major panels A-H. Expression was evaluated by confocal microscopy. Representative images of Western blot and densitometric analysis from renal cortex homogenates is shown in panel I (claudin-2) and J (occludin). Data are expressed as relative density from 3 rats/group normalized with glyceraldehyde-3-phosphate dehydrogenase (GAPDH) as loading control. Values are means±SEM. *P<0.05 vs. V; † p<0.05 vs. CIS. Bar=50 μm.

Figure 9. E-cadherin expression evaluated by confocal microscopy (panels A-D; green label). Renal cryosections of rats treated with vehicle (V, panel A), 5 mg/kg of cisplatin (CIS, panel B), 5 mg/kg of cisplatin + 200 mg/kg of curcumin (CIS+Cur, panel C) and 200 mg/kg of curcumin (Cur, panel D). Desmoplakin (DMPK; red label) was used as a marker of the distal tubule and 4', 6-diamine-2-phenylindole (DAPI; blue label) was used as a marker of nuclei. Merge image is shown in major panels A-D. Representative images of Western blots and densitometric analysis from renal cortex homogenates of E-cadherin (panel E) and β-catenina (panel F). Data are expressed as relative density from 3 rats/group normalized with glyceraldehyde-3-phosphate dehydrogenase (GAPDH) as loading control. Values are means±SEM. *P<0.05 vs. V; † p<0.05 vs. CIS. Bar=50 μm.

Figure 10. Curcumin is able to prevent several mechanisms through which cisplatin (CIS) induces renal injury in glomeruli and proximal and distal tubules. Curcumin renoprotective effects are associated with: (a) decreased kidney injury (KIM)-1 expression, apoptosis and acute tubular necrosis (ATN); (b) decreased oxidative stress by preventing loss of antioxidant enzymes (catalase, and GR), superoxide anion ($O_2^{\bullet -}$) production by a mechanism dependent on nicotinamide adenine dinucleotide phosphate (NADPH) oxidase activity (evidenced by increased expression of $p47^{phox}$ and $gp91^{phox}$ expressions), protein kinase C (PKC) β2 expression and scavenging of reactive oxygen species in glomeruli and proximal tubules; (c) by preventing CIS-induced decrement of nuclear factor erythroid-derived 2-like 2 (Nrf2), a transcription factor that regulates a wide array of genes related to detoxification and antioxidant function, which might be associated with the transforming growth factor-β1 (TGFβ1)-estimulated epithelial-to-mesenchymal transition (EMT), characterized by increased expression of collagen I and IV, and α-smooth muscle actin (α-SMA), and (d) by ameliorating CIS-induced loss of tight junction (TJ) proteins (claudin-2 and occludin), and adherens junction (AJ) protein (E-cadherin and β-catenin). GR; glutathione reductase; ROS, reactive oxygen species; SCr, plasma creatinine; BUN, blood urea nitrogen; NAG, N-acetyl-β-D-glucosaminidase; NAG, neutrophil gelatinase-associated lipocalin, family heat shock protein (Hsp70/72).

Supplementary figure legends

Supplementary Figure 1 The cisplatin-induced nephrotoxicity is dose-dependent. Different doses of cisplatin (CIS; 2.5, 5, 7.5 and 10 mg/kg) were tested to evaluate dose-dependent

toxicity. Plasma creatinine (A), blood urea nitrogen (B) and renal malondialdehyde (MDA) content (C) and decreases catalase activity (D). Values are means±SEM. *P<0.05 vs. V.

Table 1

Table 1. ROS scavenging ability of curcumin and reference compounds. Data are expressed as IC50 (μg/mL).

	$O_2^{\bullet-}$	$^1O_2$	H_2O_2	$OH^{\bullet}$	$ONOO^-$	HOCl	$ROO^{\bullet}$
Curcumin	3.9±0.5	8.6±0.4	7.4±0.3	56.2±7.8	2.3±0.2	106±5	0.35±0.03
Reference compound	3.7±0.3 (1)	576±6* (2)	136.5±9.5* (3)	67.0±7.2 (4)	9.9±1.4* (5)	75±3* (6)	1.2±0.08* (7
p	0.748	0.0016	0.0002	0.7254	0.0058	0.006	0.0006

(1)Tiron; (2) Lipoic acid; (3) Pyruvate; (4) Dimethylthiourea; (5) Penicillamine; (6) Ascorbic acid; (7) Trolox. Data are means ± SEM n= 3 experiments. Asterisk indicates statistical significance and p value is indicated below.

Table 2

Table 2. Morphological changes induced by cisplatin in kidney

Lesion	V	CIS	CIS+Cur	Cur
Apoptosis	-	+++	++	-
Acute tubular necrosis	-	+	-	-
Tubular cast	-	+++	++	-
Cell shedding	+	+++	+++	+

The severity of tubular injury was calculated semi-quantitatively in eight random subcortical periglomerular fields (magnification x200) per each rat for apoptosis, acute tubular necrosis and cast formation, using a 0 to 3 scale: 0, absence; 1+ (mild or <5 %); 2+ (moderate or 5 to 25%); 3+ (severe or >25%) of juxtamedullary proximal tubules.

Figure 1

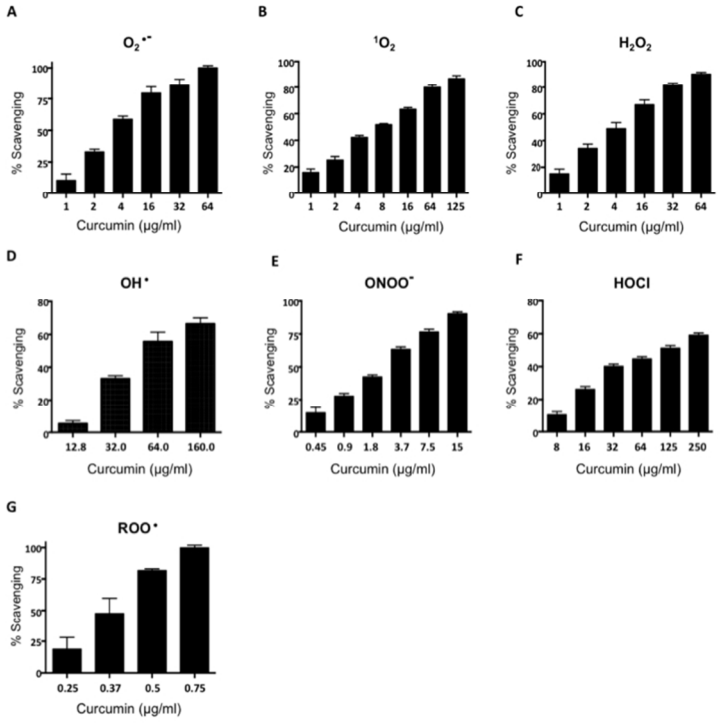

Figure 1. Curcumin scavenging activity. A: superoxide anion (O2●¯), B: singlet oxygen (1O2), C: hydrogen peroxide (H2O2), D: hydroxyl radical (OH●), E: peroxynitrite anion (ONOO¯), F: hypochlorous acid (HOCl), G: peroxyl radical (ROO●). In all scavenging assays, solutions of curcumin at different concentrations (0.25-250 µg/ml) were used; percentage of scavenging activity is shown. Data are shown as mean±SEM; n=3.
352x264mm (72 x 72 DPI)

Figure 2

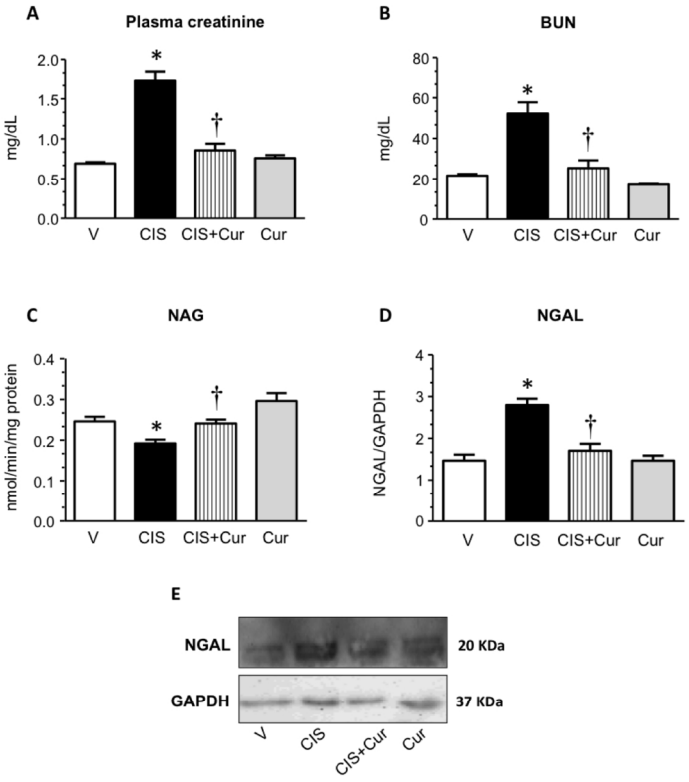

Figure 2. Renal injury markers in rats treated with vehicle (V, n=5), 5 mg/kg of cisplatin (CIS, n=9), 5 mg/kg of cisplatin + 200 mg/kg of curcumin (CIS+Cur, n=9) and 200 mg/kg of curcumin alone (Cur, n=5). (A) Plasma creatinine, (B) blood urea nitrogen (BUN), (C)N-acetyl-β-D-glucosaminidase (NAG), (D) neutrophil gelatinase-associated lipocalin (NGAL) is shown. A representative image of NGAL Western blot is shown in panel E. Data are expressed as relative density from 3 rats/group normalized with glyceraldehyde 3 phosphate dehydrogenase (GADPH) as loading control. Values are means±SEM. *P<0.05 vs. V; † p<0.05 vs. CIS.
583x486mm (72 x 72 DPI)

Figure 3

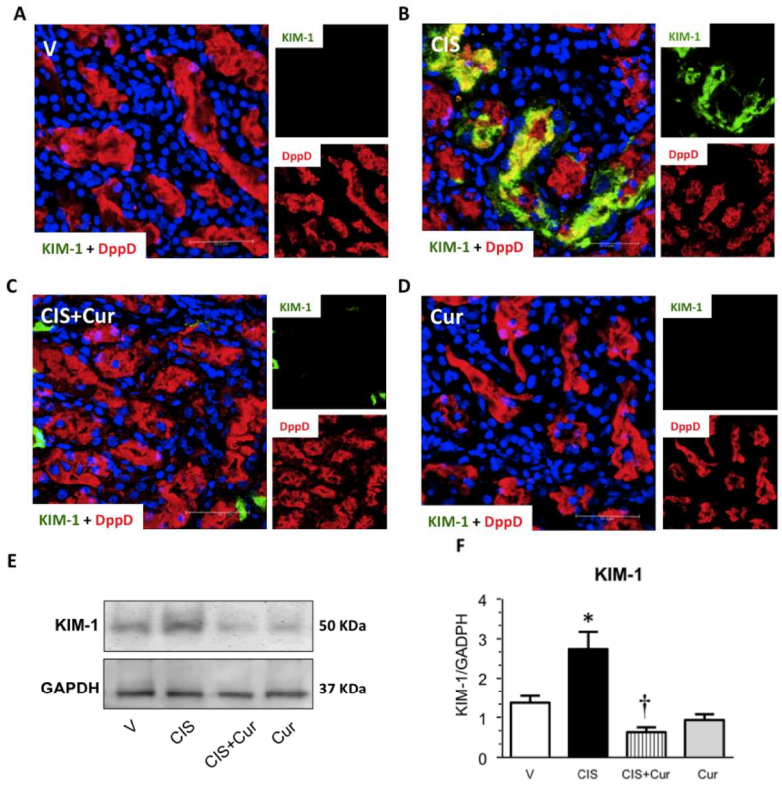

Figure 3. Kidney injury molecule-1 (KIM-1) expression was evaluated by confocal microscopy (panels A-D, green label). Representative photomicrographs of kidney layers obtained from rats treated with: vehicle group (V; panel A), 5 mg/kg of cisplatin (CIS, panel B), 5 mg/kg of cisplatin + 200 mg/kg of curcumin (CIS+Cur, panel C) and 200 mg/kg of curcumin (Cur, panel D). The expression of dipeptidyl peptidase (DppD; red label) was used as a marker of the proximal tubule apical membrane and 4', 6-diamine-2-phenylindole (DAPI; blue label) was used as a marker of the nuclei. Merge images are shown in major panels A-D. Representative Western blot for KIM-1 is shown in panel E and densitometric analyses of Western blots are shown in panel F; data are expressed as relative density from 3 rats/group normalized with glyceraldehyde-3-phosphate dehydrogenase (GAPDH) as loading control. Values are means±SEM. *P<0.05 vs. V; † p<0.05 vs. CIS. Bar=50 μm.
583x486mm (72 x 72 DPI)

Figure 4

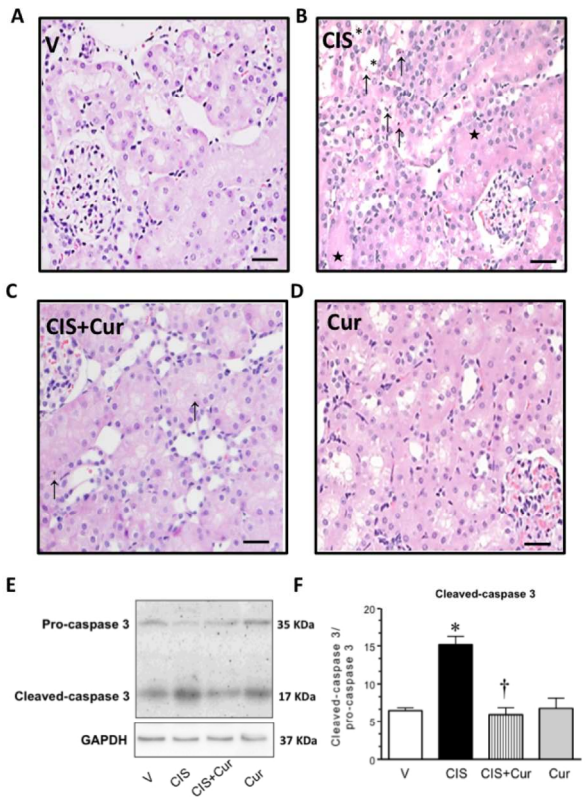

Figure 4. Representative renal light microscopy of kidney layers obtained form rats treated with (A) vehicle (V) and (B) 5 mg/kg of cisplatin (CIS). Apoptotic cells (↑), acute tubular necrosis (*) and formation of tubular casts (★) in the corticomedullary junction are shown. Additional groups of rats were treated with (C) 5 mg/kg of cisplatin + 200 mg/kg of curcumin (CIS+Cur) and (D) 200 mg/kg of curcumin (Cur). Kidney slides were stained with H&E-staining, original magnification 200x. Expression of cleaved-caspase 3 in kidney homogenates, representative western blots of pro-caspase 3 and cleaved-caspase 3 is shown in panel E, and densitometric analysis of Western blots is shown in panel F. Data are expressed as the ratio cleaved-caspase 3/pro-caspase 3 of 3 rats/group, both bands were corrected with glyceraldehyde-3-phosphate dehydrogenase (GAPDH) as loading control. Values are means±SEM. *P<0.05 vs. V; † p<0.05 vs. CIS. Bar=50 μm.
583x486mm (72 x 72 DPI)

Figure 5

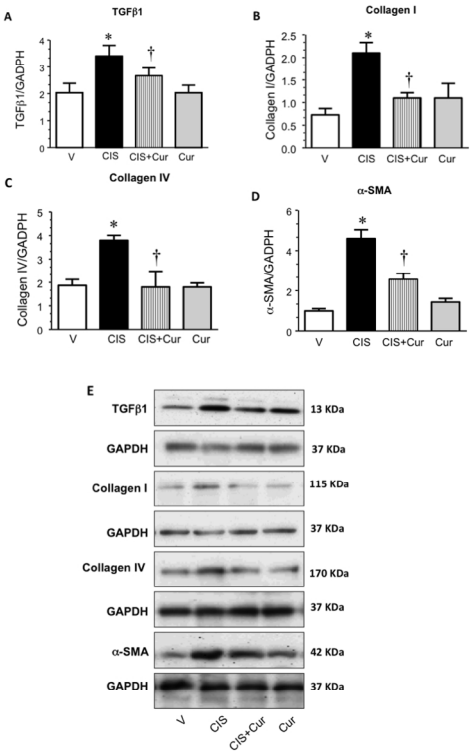

Figure 5. Proteins profibrotic factors were assessed by Western blot analysis in kidney homogenates of rats treated with vehicle (V), 5 mg/kg of cisplatin (CIS), 5 mg/kg of cisplatin + 200 mg/kg of curcumin (CIS+Cur) and 200 mg/kg of curcumin (Cur). Expression of transforming growth factor beta 1 (TGFβ1; panels A and E), collagen I (B and E), collagen IV (C and E) and alpha-smooth muscle actin (α-SMA; D and E) is shown. Representative Western blots of TGFβ1, collagen I, collagen IV, α−SMA and glyceraldehyde-3-phosphate dehydrogenase (GAPDH) are shown in panel E. Data are expressed as relative density from 3 rats/group normalized with GAPDH as a loading control, GAPDH is shown for every protein. Values are means ± SEM. *P<0.05 vs. V; † p<0.05 vs. CIS.
583x486mm (72 x 72 DPI)

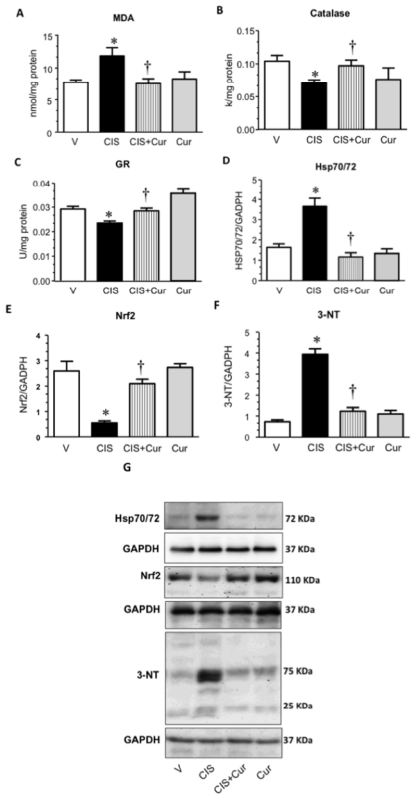

Figure 6. (A) Malondialdehyde (MDA) levels, activity of antioxidant enzymes: (B) catalase (CAT) and (C) glutathione reductase (GR), (D) family heat shock protein 70 (Hsp70/72), (E) nuclear factor erythroid-derived 2-like 2 (Nrf2), (F) expression and protein tyrosine nitration (3-NT) in renal tissue of rats treated with vehicle (V), 5 mg/kg of cisplatin (CIS), 5 mg/kg of cisplatin + 200 mg/kg of curcumin (CIS+Cur) and 200 mg/kg of curcumin (Cur). A representative Western blot images of Hsp70/72, Nrf-2, 3-NT and GADPH are shown in panel G. Data are expressed as relative density from 3 rats/group normalized with GADPH as loading control. Values are means±SEM. *P<0.05 vs. V; † p<0.05 vs. CIS.
583x486mm (72 x 72 DPI)

Figure 7

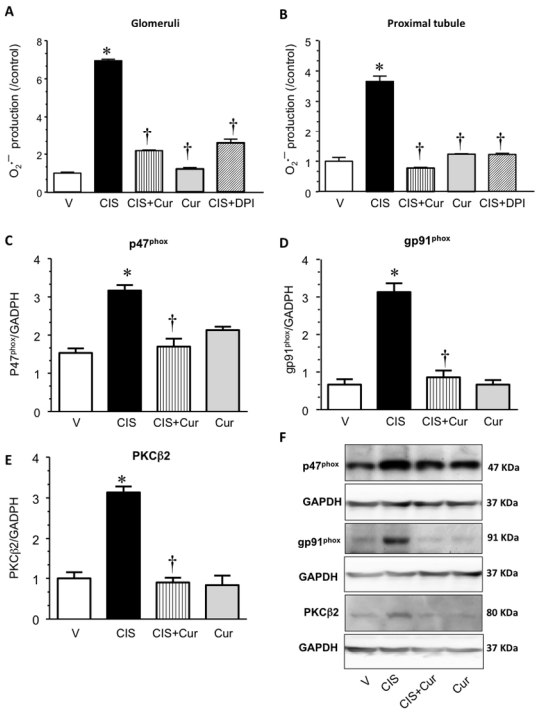

Figure 7. Superoxide anion (O2•¯) production in (A) isolated glomeruli and (B) proximal tubules and renal expression of NADPH oxidase subunits (C) p47phox and (D) gp91phox and (E) protein kinase C (PKC) β2 of rats treated with vehicle (V), 5 mg/kg of cisplatin (CIS), 5 mg/kg of cisplatin + 200 mg/kg of curcumin (CIS+Cur) and 200 mg/kg of curcumin (Cur). O2•¯ production in samples from CIS-treated rats was also evaluated in the presence of the inhibitor of the NADPH oxidase, diphenylene iodonium (DPI; bar with diagonal lines). Data are expressed as O2•¯ production (/control), n=5 rats per group. A representative Western blot image of NADPH oxidase subunits p47phox and gp91phox, PKCβ2 and GADPH are shown in panel F. Data are expressed as relative density from 3 rats/group normalized with glyceraldehyde-3-phosphate dehydrogenase (GAPDH) as a loading control each. Values are means±SEM. *P<0.05 vs. V; † p<0.05 vs. CIS.
583x486mm (72 x 72 DPI)

Figure 8

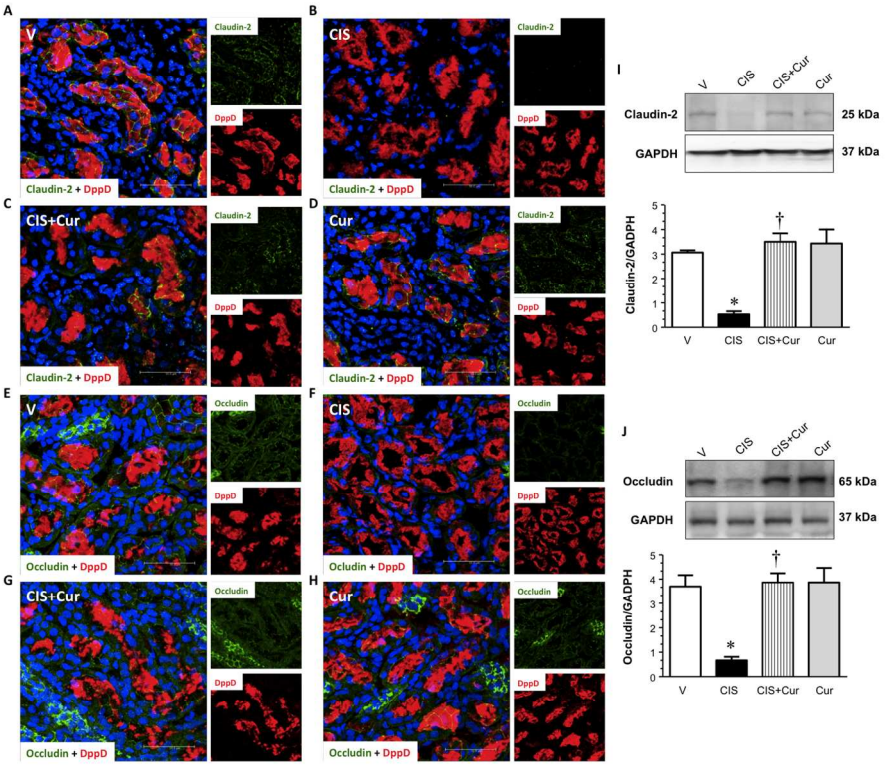

Figure 8. Immunofluorescence of kidney layers obtained from rats treated with vehicle (V, panels A and E), 5 mg/kg of cisplatin (CIS, panels B and F), 5 mg/kg of cisplatin + 200 mg/kg of curcumin (CIS+Cur, panels C and G) and 200 mg/kg of curcumin (Cur, panels D and H) of claudin-2 (panels A-D; green label) and occludin (panels E-H; green label), both proteins were detected surrounding the brush border of proximal tubular cells. Dipeptidyl peptidase (DppD; red label) was used as a marker of the proximal tubule apical membrane and 4', 6-diamine-2-phenylindole (DAPI; blue label) was used to mark nuclei. Merge image of markers is shown in major panels A-H. Expression was evaluated by confocal microscopy. Representative images of Western blot and densitometric analysis from renal cortex homogenates is shown in panel I (claudin-2) and J (occludin). Data are expressed as relative density from 3 rats/group normalized with glyceraldehyde-3-phosphate dehydrogenase (GAPDH) as loading control. Values are means±SEM. *P<0.05 vs. V; † p<0.05 vs. CIS. Bar=50 μm.
583x486mm (72 x 72 DPI)

Figure 9

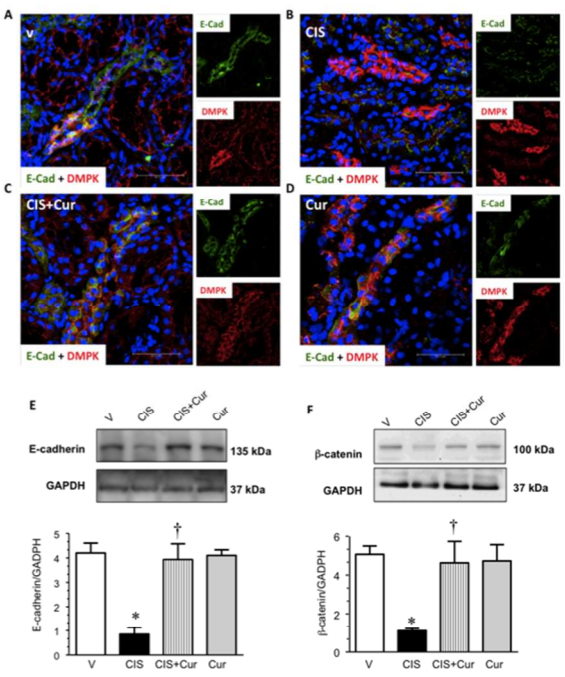

Figure 9. E-cadherin expression evaluated by confocal microscopy (panels A-D; green label). Renal cryosections of rats treated with vehicle (V, panel A), 5 mg/kg of cisplatin (CIS, panel B), 5 mg/kg of cisplatin + 200 mg/kg of curcumin (CIS+Cur, panel C) and 200 mg/kg of curcumin (Cur, panel D). Desmoplakin (DMPK; red label) was used as a marker of the distal tubule and 4', 6-diamine-2-phenylindole (DAPI; blue label) was used as a marker of nuclei. Merge image is shown in major panels A-D. Representative images of Western blots and densitometric analysis from renal cortex homogenates of E-cadherin (panel E) and β-catenina (panel F). Data are expressed as relative density from 3 rats/group normalized with glyceraldehyde-3-phosphate dehydrogenase (GAPDH) as loading control. Values are means±SEM. *P<0.05 vs. V; † p<0.05 vs. CIS. Bar=50 μm.
352x264mm (72 x 72 DPI)

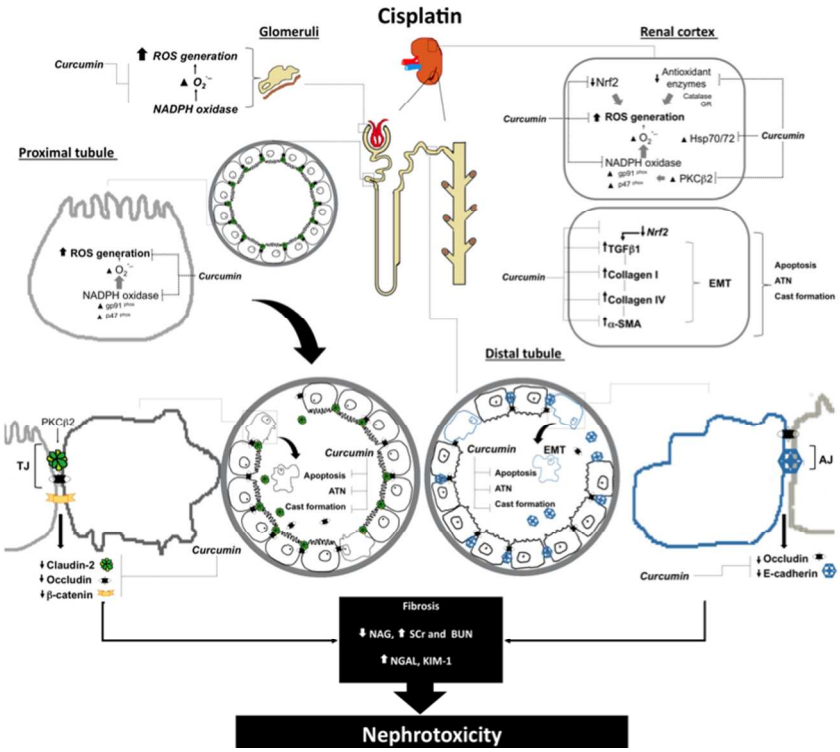

Figure 10. Curcumin is able to prevent several mechanisms through which cisplatin (CIS) induces renal injury in glomeruli and proximal and distal tubules. Curcumin renoprotective effects are associated with: (a) decreased kidney injury (KIM)-1 expression, apoptosis and acute tubular necrosis (ATN); (b) decreased oxidative stress by preventing loss of antioxidant enzymes (catalase, and GR), superoxide anion ($O_2^{\bullet -}$) production by a mechanism dependent on nicotinamide adenine dinucleotide phosphate (NADPH) oxidase activity (evidenced by increased expression of p47phox and gp91phox expressions), protein kinase C (PKC) β2 expression and scavenging of reactive oxygen species in glomeruli and proximal tubules; (c) by preventing CIS-induced decrement of nuclear factor erythroid-derived 2-like 2 (Nrf2), a transcription factor that regulates a wide array of genes related to detoxification and antioxidant function, which might be associated with the transforming growth factor-β1 (TGFβ1)-estimulated epithelial-to-mesenchymal transition (EMT), characterized by increased expression of collagen I and IV, and α-smooth muscle actin (α-SMA), and (d) by ameliorating CIS-induced loss of tight junction (TJ) proteins (claudin-2 and occludin), and adherens junction (AJ) protein (E-cadherin and β-catenin). GR; glutathione reductase; ROS, reactive oxygen species; SCr, plasma creatinine; BUN, blood urea nitrogen; NAG, N-acetyl-β-D-glucosaminidase; NAG, neutrophil gelatinase-associated lipocalin, family heat shock protein (Hsp70/72).
352x264mm (72 x 72 DPI)

Supplementary figure 1

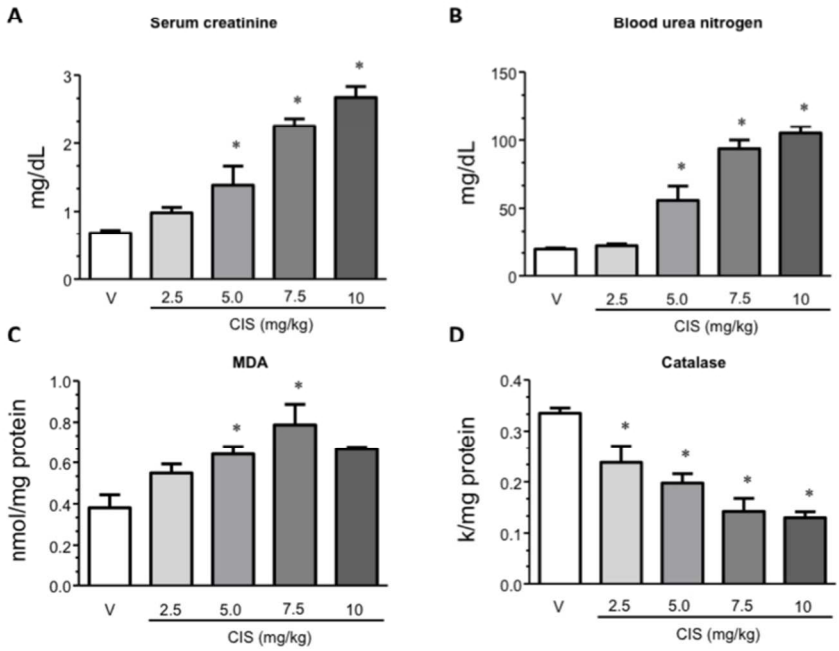

Supplementary Figure 1 The cisplatin-induced nephrotoxicity is dose-dependent. Different doses of cisplatin (CIS; 2.5, 5, 7.5 and 10 mg/kg) were tested to evaluate dose-dependent toxicity. Plasma creatinine (A), blood urea nitrogen (B) and renal malondialdehyde (MDA) content (C) and decreases catalase activity (D). Values are means±SEM. *P<0.05 vs. V.
352x264mm (72 x 72 DPI)